IOP Publishing Physics in Medicine and Biology

Phys. Med. Biol. **53** (2008) 295–304 doi:10.1088/0031-9155/53/1/021

Temporal variation of dielectric properties of preserved blood

Yoshihito Hayashi[1], Ikuya Oshige[1], Yoichi Katsumoto[1], Shinji Omori[1], Akio Yasuda[1] and Koji Asami[2]

[1] Life Science Laboratory, Materials Laboratories, Sony Corporation, Sony Bioinformatics Center, Tokyo Medical and Dental University, Bunkyo-ku, Tokyo 113-8510, Japan
[2] Laboratory of Molecular Aggregation Analysis, Division of Multidisciplinary Chemistry, Institute for Chemical Research, Kyoto University, Uji, Kyoto 611-0011, Japan

E-mail: Yoshihito.Hayashi@jp.sony.com

Received 28 September 2007, in final form 22 November 2007
Published 19 December 2007
Online at stacks.iop.org/PMB/53/295

Abstract

Rabbit blood was preserved at 277 K in Alsever's solution for 37 days, and its dielectric permittivity was monitored in a frequency range from 0.05 to 110 MHz throughout the period. The relaxation time and Cole–Cole parameter of the interfacial polarization process for erythrocytes remained nearly constant during the first 20 days and then started to increase and decrease, respectively. On the other hand, the relaxation strength and the cell volume fraction continued to decrease for 37 days, but the decrease rates of both changed discontinuously on about the 20th day. Microscope observation showed that approximately 90% of the erythrocytes were spinous echinocytes at the beginning of preservation and started to be transformed into microspherocytes around the 20th day. Therefore, dielectric spectroscopy is a sensitive tool to monitor the deterioration of preserved blood accompanied by morphological transition of erythrocytes through the temporal variation of their dielectric properties.

1. Introduction

Quality of blood is critical for both clinical use (transfusion) and industrial use (blood products). For example, non-immunological side effects upon transfusion brought about by poor quality of blood include (1) hyperthermia and sepsis attributed to bacterial contamination of blood, (2) hyperkalemia due to hemolysis of preserved erythrocytes and potassium leakage from them, (3) virus infection of blood and so on (García-Erce *et al* 2000, Ramirez *et al* 1987, Thorp *et al* 1990, Frei and Fleisch 1961). Although blood is tested after it is collected, it is not necessarily in the perfect condition when used even within a certain shelf life. Considering the seriousness of the matter, a continuous effort for the development of simple and fast blood tests is required.

Dielectric spectroscopy (DS) is a nondestructive, label-free method to investigate heterogeneous systems such as blood cell suspensions. The complex permittivity for such a system as a function of frequency of the applied electric field exhibits a large dielectric relaxation called β-dispersion in the megahertz region, which is attributed to the interfacial polarization process (Hanai 1968, Foster and Schwan 1989, Takashima 1989, Asami 1998, Asami *et al* 1999, Bordi *et al* 2001a, Feldman *et al* 2003). Thus, the dispersion curve is sensitive to geometric and electric changes in blood cells. Therefore, we expect that DS can be an important principle for simple, fast automated blood-test systems. Indeed, Bordi *et al* (2001b) found that the dielectric properties of human erythrocyte membrane changed through blood storage, although their DS study was performed only for the first 13 days of storage, while it was claimed that erythrocytes can be stored in the buffer used for the study for 9–10 weeks without significant deterioration. Thus, little is known as to how the dielectric properties of blood change along with blood deterioration during longer preservation.

Suspensions of spherical erythrocytes artificially swollen by hypotonic buffer and spherical erythrocyte ghosts were investigated by DS (Asami *et al* 1989, Kaneko *et al* 1991, Caduff *et al* 2004). Experimental complex permittivity (ε^*) for such a suspension can be described by the Maxwell–Wagner mixture formula if the cell volume fraction (ϕ) is not very high (typically $\phi \leqslant 0.3$ for erythrocytes):

$$\varepsilon^* = \varepsilon_a^* \frac{(2\varepsilon_a^* + \varepsilon_p^*) - 2\phi(\varepsilon_a^* - \varepsilon_p^*)}{(2\varepsilon_a^* + \varepsilon_p^*) + \phi(\varepsilon_a^* - \varepsilon_p^*)}, \tag{1}$$

while Hanai's mixture formula (Asami *et al* 1989) is more accurate for higher ϕ:

$$\frac{\varepsilon^* - \varepsilon_p^*}{\varepsilon_a^* - \varepsilon_p^*} \left(\frac{\varepsilon_a^*}{\varepsilon^*}\right)^{\frac{1}{3}} = 1 - \phi, \tag{2}$$

where ε_a^* is the complex permittivity of a surrounding medium and ε_p^* is that of a cell, which is given by the single-shell model as a function of permittivity and conductivity of the cell membrane (ε_m and κ_m, respectively), those of the cytoplasm (ε_i and κ_i, respectively), diameter of the cell (D) and thickness of the membrane (d) as discussed in detail elsewhere (Kaneko *et al* 1991):

$$\varepsilon_p^* = \varepsilon_m^* \frac{2(1-v)\varepsilon_m^* + (1+2v)\varepsilon_i^*}{(2+v)\varepsilon_m^* + (1-v)\varepsilon_i^*}, \tag{3a}$$

$$v = \left(\frac{D}{D+2d}\right)^3, \tag{3b}$$

and

$$\varepsilon_x^* = \varepsilon_x - j\frac{\kappa_x}{\omega\varepsilon_0}, \tag{3c}$$

where subscript $x = a$, m and i, and ε_a and κ_a are the permittivity and conductivity of the surrounding medium, respectively. Therefore, these cell phase parameters can be estimated from the DS data for a suspension of spherical cells (Kaneko *et al* 1991, Caduff *et al* 2004).

In the present work, we performed DS measurements for preserved rabbit blood for 37 days to monitor the change in its dielectric permittivity and discuss the mechanism for the change. A microscope observation was simultaneously performed to relate the morphological transition of erythrocytes to the permittivity change, and measured cell sizes were used for quantitative analysis of the DS data based on the single-shell model. Note that the average lifetime of rabbit erythrocytes *in vivo* (about 60 days) is much shorter than that of human erythrocyte (about 120 days). Thus, it is expected that rabbit blood deteriorates more rapidly

also *in vitro* than human blood. Indeed, owing to this experimental advantage, we successfully monitored the dielectric permittivity until blood was clearly deteriorated and found not only gradual but also abrupt change in the permittivity. We do not claim that the results of our work are readily applicable to human blood because of different dielectric properties of rabbit and human blood, but the methodology developed here is the basis for future extension over human blood.

2. Materials and methods

Blood of a healthy rabbit (*Oryctolagus cuniculus*, about 15 weeks old), which was collected in an antiseptic environment and immediately mixed with the equal volume of Alsever's solution (anhydrous citric acid 0.55 g l^{-1}, anhydrous sodium citrate 8.0 g l^{-1}, sodium chloride 4.2 g l^{-1} and glucose 20.5 g l^{-1}), was supplied from Kohjin Bio Co. Ltd (Japan) one day after it was collected. This blood (pH 6.8) was stored at 277 K and shaken for 1 min in an antiseptic environment just before its small portion of 1.5 ml was sampled by a syringe for each measurement. The sampled blood was stored in a micro tube at room temperature (298 K) for 20 min and used for both DS and microscope measurements immediately after shaking the micro tube for 15 s.

DS measurements in a frequency range from 40 Hz to 110 MHz were performed without further sample treatment using an impedance analyzer (Agilent model 4294A). The sample holder used in this study is a capacitor-type one that consists of two parallel platinum electrodes with the spacing of 3.5 mm and the diameter of 8 mm, and the required volume of sample is 160 μl. The electrodes were carefully plated with platinum black to reduce the parasitic capacitance due to the electrode polarization (Asami *et al* 1984, Omori *et al* 2006, Katsumoto *et al* 2007). The temperature of the sample holder was controlled at 298 K by water circulation. Measurement time was about 4 min including waiting time for stabilization of the sample temperature. Note that the sedimentation of erythrocytes was negligible for this measurement time. The effects of the residual inductance and stray capacitance were corrected for by the previously reported method (Asami *et al* 1984). Simultaneously, digital images of erythrocytes from the same micro tube were taken by an optical microscope (Carl Zeiss model Axio Imager M1). This measurement took less than 10 min. In our digital-image processing, 400–1000 cells randomly chosen were classified into different types of erythrocytes to determine their populations. Among them, more than 30 cells of each type were randomly chosen for size measurement with a standard error of less than 3%.

3. Results and discussion

Approximately 90% of erythrocytes were echinocytes when we received the blood sample, as shown in a scanning electron microscope (SEM) image of figure 1(a), although normal rabbit erythrocytes have a biconcave-disk shape similar to that of human erythrocytes. We recall here that although echinocytes are known to be frequently found in the blood of uremic patients (Zachée *et al* 1994, Agroyannis *et al* 2001), even healthy erythrocytes are also transformed *in vitro* into echinocytes as a consequence of high pH (Gedde *et al* 1997) or sustained preservation (Högman *et al* 1980). Thus, we consider that dominance of echinocytes is probably due to the temporal transformation of normal erythrocytes during preservation before the blood was received. Our microscope observation showed that the population of normal erythrocytes was less than 10% throughout preservation.

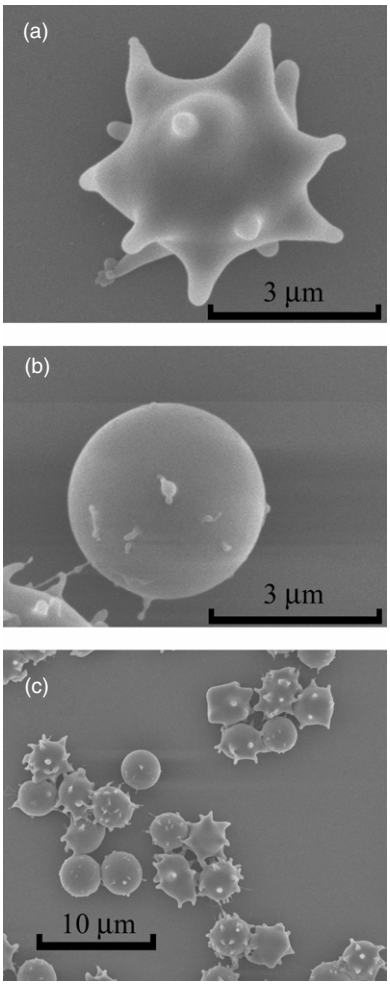

Figure 1. SEM images of (a) an echinocyte, (b) a microspherocyte and (c) the mixture of them. Note that the erythrocytes were reduced owing to the dehydration process after they were fixed by 1% glutaraldehyde for SEM imaging. Thus, we did not use the SEM images for size measurement in figure 2.

Microspherocytes were also found (figures 1(b) and (c)). Note that the average diameter of the microspherocytes (4.5 μm) is much smaller than that of the spherocytes artificially prepared in hypotonic 65% phosphate-buffered saline (PBS) and in more acidic PBS of pH 5.3 (6.9 and 6.1 μm, respectively). Hence, microspehrocytes and spherocytes can easily be discriminated. The population of the microspherocytes started to increase on about the 20th day from blood collection, as shown in figure 2(a). The outer diameter of the echinocytes, which is defined as the top-to-top distance between a diagonal pair of spines, decreased during preservation, as shown in figure 2(b). In contrast, the inner diameter, which is defined as the valley-to-valley distance, remained constant at about 4.3 μm and is very close to the average diameter of the microspherocytes (figure 2(b)). This means that only the length of the spines continued to decrease. Moreover, the spines were found to get thinner during preservation, although it was difficult to quantify the change by microscope observation. Therefore, some

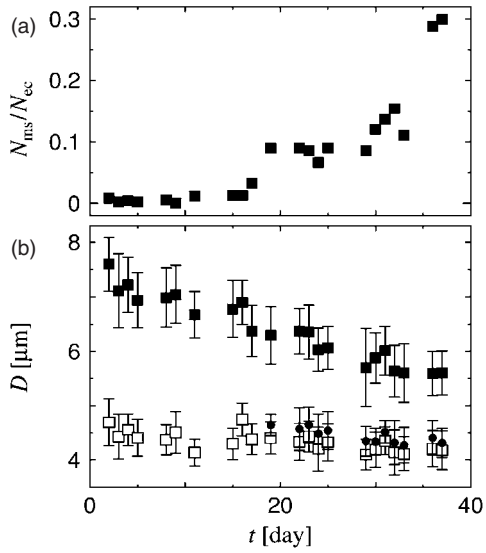

Figure 2. (a) Ratio of the number of microspherocytes N_{ms} to that of echinocytes N_{ec} against the period of blood preservation and (b) the diameters of echinocytes corresponding to the top-to-top and valley-to-valley distances for a diagonal pair of spines (full and open boxes, respectively), and the diameter of microspherocytes (full circles). Error bars show standard deviation.

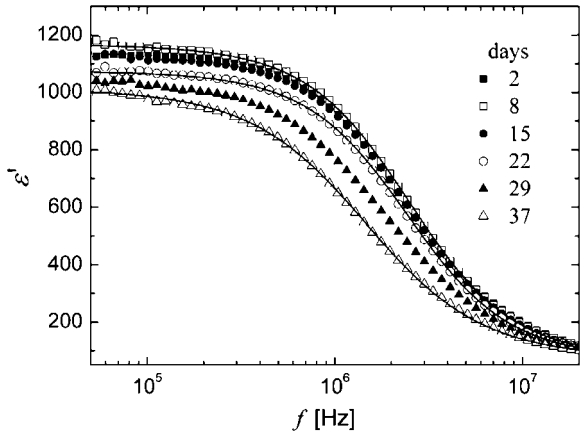

Figure 3. Representative dielectric dispersion curves of the preserved rabbit blood after various preservation periods from 2 to 37 days. The symbols show the experimental data, and the solid curves are the fitting functions of equation (4) after 8, 22 and 37 days.

of the echinocytes were transformed to the microspherocytes during preservation, so that deterioration of blood is accompanied by morphological change of erythorocytes.

The dielectric spectra demonstrated the large relaxation as shown in figure 3, where only the data in the frequency range corresponding to β-dispersion were presented. It is qualitatively seen that the relaxation strength and the characteristic frequency continuously

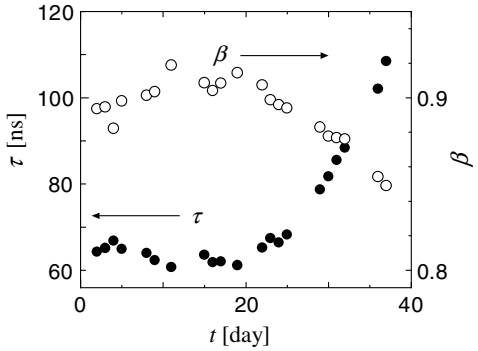

Figure 4. Relaxation time τ (full circles) and the Cole–Cole parameter β (open circles) obtained by curve fitting with equation (4) against the period of blood preservation.

decreased during preservation. For more quantitative data analysis of ε^*, we carried out curve fitting to the experimental data with a single Cole–Cole function given by

$$\varepsilon^* - \varepsilon_\infty = \frac{\Delta\varepsilon}{1 + (\mathrm{j}\omega\tau)^\beta} + \frac{\kappa_\mathrm{l}}{\mathrm{j}\varepsilon_0\omega}, \tag{4}$$

where j is the imaginary unit, ω is the angular frequency, $\Delta\varepsilon$ is the relaxation strength, τ is the relaxation time, β is the Cole–Cole parameter that introduces the symmetrical broadening of the relaxation function, κ_l is the dc conductivity, ε_0 is the permittivity of vacuum and ε_∞ is the permittivity in the high-frequency limit. The experimental data were well described by equation (4), as shown in figure 3.

As a function of preservation time, τ and β started to respectively increase and decrease on about the 20th day, as shown in figure 4. Our microscope observation showed that the number of the microspherocytes also started to increase at this point (figure 2(a)), while the outer diameter of the echinocytes continued to decrease during preservation (figure 2(b)). It seems at first sight that the reduction of the average cell size leads to the decrease of τ, but interestingly, the experimental data show the opposite trend. Figure 5 shows that $\Delta\varepsilon$ decreased continuously during preservation. The slope, however, changed on about the 20th day and got steeper after this point, although the variance of the data is larger than that for τ and β. The relaxation strength of the interfacial polarization depends on ϕ, which can be estimated according to Hanai's theory (Asami *et al* 1989) as

$$\phi = 1 - \left(\frac{\kappa_\mathrm{l}}{\kappa_\mathrm{a}}\right)^{\frac{2}{3}}. \tag{5}$$

In practice, the conductivities of the suspension and the supernatant of the suspension after centrifugation measured at 11 kHz were respectively used for κ_l and κ_a to calculate ϕ. The value of κ_a was 1.22 S m^{-1} and did not change during the preservation period. Equation (5) is applicable to a suspension of nonconductive spheres. Since β-dispersion appears in much higher frequencies, erythrocytes can be considered to be nonconductive at 11 kHz. Even though the effects of spines on the echinocytes are not included in the theory, we employed equation (5) to give approximate values of ϕ. As shown in figure 5, ϕ decreased along with the preservation date, and the slope grew steeper about the 20th day; this is very similar to the variation of $\Delta\varepsilon$.

Now we turn to discuss the mechanism of the increase of τ after about 20 days of preservation. According to the theory of the interfacial polarization for cell suspensions

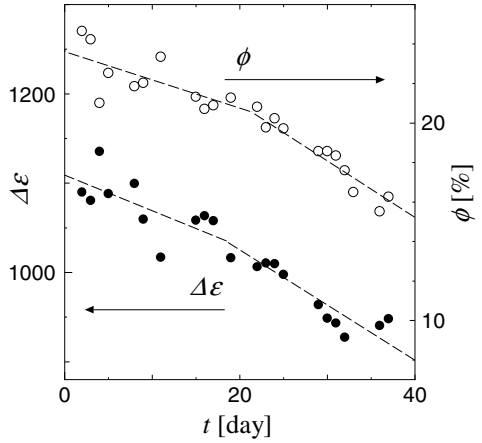

Figure 5. Relaxation strength $\Delta\varepsilon$ (full circles) obtained by curve fitting with equation (4) and the cell volume fraction ϕ estimated by equation (5) (open circles) against the period of blood preservation.

(Takashima 1989), increase of τ is induced by decrease of the cytoplasm conductivity κ_i (case 1) and increase of the specific cell membrane capacitance ($C_m = \varepsilon_0\varepsilon_m/d$) (case 2). In case 2, however, $\Delta\varepsilon$ should also increase, but this is contradictory to the experimental result. To account for the increase of τ in case 2, therefore, simultaneous changes of other parameters that induce the decrease of $\Delta\varepsilon$ must be considered, which include decrease of D (case 2a), decrease of ϕ (case 2b) and increase of κ_m (case 2c).

To figure out the most reasonable mechanism among the four cases above, numerical estimation of cell phase parameters (D, ϕ, ε_m, C_m and κ_i) on the basis of equation (1) with the simplified spherical cell model is useful as an approximation in the present case. In this estimation, the values of τ and $\Delta\varepsilon$ obtained by fitting equation (4) to the experimental dispersion curves for 8 and 37 days of preservation were used for models A and B corresponding to the data before and after the abrupt increase of τ on the 20th day, respectively. Pauly and Schwan (1959) showed that equation (1) for a cell suspension can be rewritten as a Debye-type relaxation function. According to this relationship, three of the cell phase parameters are analytically obtainable, if the other parameters are known, by using the experimental values of τ, $\Delta\varepsilon$ and κ_l. Note that even though we used the Cole–Cole function of equation (4) for data fitting to extract τ and $\Delta\varepsilon$ because of the broadening of the relaxation due to size and shape distribution of erythrocytes including variety of spines on the surfaces of echinocytes, the relations between those experimental parameters and the cell phase parameters should not be very different from those for the spherical cell model. Thus, we kept $\kappa_a = 1.22$ S m^{-1}, $\varepsilon_a = 78.36$ and $\varepsilon_i = 60$ (Asami *et al* 1989, Caduff *et al* 2004) for all the four cases (note that ε^* is not very sensitive to ε_i (Polevaya *et al* 1999)), and the estimation was performed as follows.

First, for model A, D was fixed at the values of the inner and outer diameters of the echinocytes experimentally determined, and ϕ, C_m and κ_i were obtained (rows 1 and 2 in table 1, respectively). The value of κ_m was assumed to be zero as usual for living cells (Takashima *et al* 1988, Caduff *et al* 2004). Second, the value of κ_i as obtained for model A was used for model B, and D, ϕ and C_m were regarded as unknown variables to be solved. Among them, ϕ was independently obtainable from κ_l and κ_a. Thus, simultaneous equations of D and C_m including τ and $\Delta\varepsilon$ as parameters were set up. However, they were found to

Table 1. Geometric and cell phase parameters for spherical cell suspension models.

No.	D (μm)	ϕ	κ_m (S m^{-1})	C_m (mF m^{-2})	κ_i (S m^{-1})
			Model A		
1	4.37[a,b]	0.230	0[a]	10.9	0.439
2	6.99[a,c]	0.230	0[a]	6.82	0.439
			Model B		
3	4.18[a,b]	0.169	0[a]	12.7	0.270
4	5.60[a,c]	0.169	0[a]	9.44	0.269
5	4.18[a,b]	0.220	9.07×10^{-4}	39.6	0.439[a]
6	5.60[a,c]	0.220	6.76×10^{-4}	29.6	0.439[a]

[a] Given parameter (not estimated parameter).
[b] Average inner diameter of the echinocytes obtained by the microscope observation.
[c] Average outer diameter of the echinocytes obtained by the microscope observation.

be contradictory, and thus there were no solutions. Therefore, cases 2a and 2b were rejected. Third, the assumption of $\kappa_m = 0$ was removed (rows 5 and 6 in table 1). This numerical estimation for case 2c gave the κ_m value of about $7 \sim 9 \times 10^{-4}$ S m^{-1} and striking increases of C_m. Because the plasma membranes of dead cells lose the barrier to the flow of ions, increases of κ_m with blood deterioration may occur. However, it is difficult to explain the increase of C_m by factors of more than three as compared with model A. Nevertheless, we do not rule out case 2c completely because our consideration does not take into account change of spines on the surfaces of echinocytes that may affect C_m.

After the discussion above, we conclude that case 1, i.e., decrease of κ_i is the most probable mechanism for the change of τ with blood storage (compare rows 1 and 2 with rows 3 and 4 in table 1, respectively). Note that κ_a (1.22 S m^{-1}) was much higher than κ_i (0.44 S m^{-1} for model A)—this is consistent with the previous studies (Asami *et al* 1980, Livshits *et al* 2007). Thus, it is not likely that ion leakage caused the reduction of κ_i. Change in the ionic constituents induced by outflow of potassium ions and inflow of sodium ions could contribute to the decrease of κ_i. However, this effect alone cannot account for large increase of τ because the difference of molar conductivity between sodium chloride and potassium chloride is relatively small (about 20%). Hence, it is reasonable to consider that the proteins (mainly hemoglobin) inside erythrocytes have some effects. If the protein concentration increases as a result of the cell size reduction, the viscosity of the cytoplasm increases, and thus the diffusion constants of ions decrease and this leads to the lower κ_i. This model, however, cannot account for the abrupt increase of τ on the 20th day despite of the continuous decrease of the echinocyte size from the beginning of preservation. Here, we refer to the previous report that heat denaturation and subsequent gelation of protein cause significant reduction of the conductivity of the system (Hayashi *et al* 2000). Thus, we consider that protein denaturation and possibly aggregation started in the cytoplasm after about 20 days that reduced the diffusion constants of ions remarkably. Because the number of microspherocytes also started to increase on the 20th day, such change in the cytoplasm could be related to the formation of the microspherocytes. With the increase of the microspherocyte population, the heterogeneity of the suspension increases; this accounts for the decrease of β.

Finally, we discuss possible reasons of decreasing ϕ and $\Delta\varepsilon$ with blood preservation. One is the shortening of the spines on the echinocytes. However, the rate of the shortening did not change during preservation; no change of the decrease rate is observed about the 20th day in figure 2(b). Instead, the increase of the microspherocyte population is probably responsible

for the changes of ϕ and $\Delta\varepsilon$ on the 20th day, as the transformation from the echinocytes to the microspherocytes causes the reduction of these parameters. However, we do not exclude the possibility that the decreases of ϕ and $\Delta\varepsilon$ could also reflect the reduction of the cell number concentration due to hemolysis or other factors that we have not noticed yet.

In conclusions, the present work showed that the dielectric response of the preserved rabbit blood clearly changed at a certain critical point, about the 20th day from blood collection. This change was accompanied by morphological transition of erythrocytes. Moreover, the increase of the relaxation time indicates the reduction of cytoplasm conductivity probably related to the change in the molecular structure of protein and the ionic constituents inside the cells. Therefore, blood deterioration in this study involved correlated morphological and electric changes of erythrocytes, and DS with the microscope observation revealed the mechanism.

References

Agroyannis B, Kopelias I, Fourtounas C, Paraskevopoulos A, Tzanatos H, Dalamangas A and Mallas E 2001 Relation between echinocytosis and erythrocyte calcium content in hemodialyzed uremic patients *Artif. Organs* **25** 486–502

Asami K 1998 Dielectric relaxation spectroscopy of biological cell suspensions *Handbook on Ultrasonic and Dielectric Characterization Techniques for Suspended Particulates* ed V A Hackley and J Texter (Westerville: The American Ceramic Society) pp 333–49

Asami K, Hanai T and Koizumi N 1980 Dielectric approach to suspensions of ellipsoidal particles covered with a shell in particular reference to biological cells *Japan. J. Appl. Phys* **19** 359–65

Asami K, Irimajiri A, Hanai T, Shiraishi N and Utsumi K 1984 Dielectric analysis of mitochondria isolated from rat liver I. Swollen mitoplasts as simulated by a single-shell model *Biochim. Biophys. Acta* **778** 559–69

Asami K, Takahashi Y and Takashima S 1989 Dielectric properties of mouse lymphocytes and erythrocytes *Biochim. Biophys. Acta* **1010** 49–55

Asami K, Gheorghiu E and Yonezawa T 1999 Real-time monitoring of yeast cell division by dielectric spectroscopy *Biophys. J.* **76** 3345–8

Bordi F, Cametti C and Gili T 2001a Reduction of the contribution of electrode polarization effects in the radiowave dielectric measurements of highly conductive biological cell suspensions *Bioelectrochemistry* **54** 53–61

Bordi F, Cametti C, Luca F D, Gili T, Misasi R, Sorice M, Circella A and Garofalo T 2001b Structural alteration of erythrocyte membrane during storage: a combined electric conductometric and flow-cytometric study *Z. Naturforsch.* **56c** 857–64

Caduff A, Livshits L, Hayashi Y and Feldman Y 2004 Cell membrane response on d-glucose studied by dielectric spectroscopy. Erythrocyte and ghost suspensions *J. Phys. Chem.* B **108** 13827–30

Feldman Y, Ermolina I and Hayashi Y 2003 Time domain dielectric spectroscopy study of biological systems *IEEE Trans. Dielectr. Insul.* **10** 728–53

Foster K R and Schwan H P 1989 Dielectric properties of tissues and biological materials: a critical review *Crit. Rev. Biomed. Eng.* **17** 25–104

Frei P C and Fleisch A 1961 New method permitting a decrease in hemolysis of conserved blood *Helv. Physiol. Pharmacol. Acta* **19** C19–22 (article in French)

García-Erce J A, Grasa J M, Solano V M, Seoane A and Giralt M 2000 Bacterial contamination of blood components *Vox Sang* **79** 249–50

Gedde M M, Davis D K and Huestis W H 1997 Cytoplasmic pH and human erythrocyte shape *Biophys. J.* **72** 1234–46

Hanai T 1968 Electric properties of emulsions *Emulsion Science* ed P Sherman (London: Academic) pp 353–478

Hayashi Y, Miura N, Shinyashiki N, Yagihara S and Mashimo S 2000 Globule-coil transition of denatured globular protein investigated by a microwave dielectric technique *Biopolymers* **54** 388–97

Högman C F, Arro E and Hedlund K 1980 Red blood cell preservation in protein-poor media. 2. Studies of changes in red cell shape during storage *Haematologia (Budap)* **13** 135–44

Kaneko H, Asami K and Hanai T 1991 Dielectric analysis of sheep erythrocyte ghost. Examination of applicability of dielectric mixture equations *Colloid Polym. Sci.* **269** 1039–44

Katsumoto Y, Omori S, Yamamoto D, Yasuda A and Asami K 2007 Dielectric dispersion of short-stranded DNA in aqueous solutions with and without added salt *Phys. Rev.* E **75** 011911

Livshits L, Caduff A, Talary M S and Feldman Y 2007 Dielectric response of biconcave erythrocyte membranes to d- and l-glucose *J. Phys. D: Appl. Phys.* **40** 15–9

Omori S, Katsumoto Y, Yasuda A and Asami K 2006 Dielectric dispersion for short double-strand DNA *Phys. Rev.* E **73** 050901

Pauly H and Schwan H P 1959 Über die impedanz einer suspension von kugelförmigen teilchen mit einer schale *Z. Naturforsch.* **14b** 125–31

Polevaya Y, Ermolina I, Schlesinger M, Ginzburg B-Z and Feldman Y 1999 Time domain dielectric spectroscopy study of human cells II. Normal and malignant white blood cells *Biochim. Biophys. Acta* **1419** 257–71

Ramirez A M, Woodfield D G, Scott R and McLachlan J 1987 High potassium levels in stored irradiated blood *Transfusion* **27** 444–5

Takashima S 1989 *Electric Properties of Biopolymers and Membranes* (Bristol: Adam Hilger)

Takashima S, Asami K and Takahashi Y 1988 Frequency domain studies of impedance characteristics of biological cells using micropipette technique I. Erythrocyte *Biophys. J.* **54** 995–1000

Thorp J A, Plapp F V, Cohen G R, Yeast J D, O'Kell R T and Stephenson S 1990 Hyperkalemia after irradiation of packed red blood cells: possible effects with intravascular fetal transfusion *Am. J. Obst. Gynecol.* **163** 607–9

Zachée P, Boogaerts M, Snauwaert J and Hellemans L 1994 Imaging uremic red blood cells with the atomic force microscope *Am. J. Nephrol.* **14** 197–200